Journal of Membrane Science, 87 (1994) 35–46
Elsevier Science B.V., Amsterdam

A comparative study of techniques used for porous membrane characterization: pore characterization*

K.J. Kim[a], A.G. Fane[a,**], R. Ben Aim[b], M.G. Liu[b], G. Jonsson[c], I.C. Tessaro[c], A.P. Broek[d] and D. Bargeman[d]

[a]*Centre for Membrane Science and Technology, School of Chemical Engineering and Industrial Chemistry, University of New South Wales, P.O. Box 1, Kensington, N.S.W. 2033 (Australia)*
[b]*Department de Genie Chimique, Université de Technologie de Compiègne, BP649-60206 Compiègne (France)*
[c]*Department of Chemical Engineering, Technical University of Denmark, Building 229, DK2800 Lyngby (Denmark)*
[d]*Department de Chemical Technology, Twente University of Technology, P.O. Box 217, 7500 AE Enschede (Netherlands)*

(Received December 21, 1992; accepted in revised form March 17, 1993)

Abstract

A range of commercial UF membranes have been characterized by thermoporometry, biliquid permporometry and molecular weight cut-off experiments. A comparison of results from these three independent techniques for the same types of membrane shows an indication of the strength and weakness of the methods. MWCO values determined from actual rejection values using PEG and dextran were significantly lower than the manufacturer supplied data. The data obtained using the biliquid permporometry and solute rejection tests produced contrasting results for Amicon polysulfone (PM30) and regenerated cellulose (YM30) membranes. While MWCO determination resulted in sharper cut-off curves, the biliquid permporometry offered a broader size distribution with the PM30 and *vice versa* with the YM30. The pore sizes obtained by thermoporometry were significantly larger than those by the biliquid permporometry. The biliquid permporometry and thermoporometry give significantly higher values than the MWCO method. The closest comparison is obtained between the EM values and the MWCO method. This suggests that the controlling pore dimension for separation is the surface skin dimension.

Key words: ultrafiltration; pore characterization; molecular weight cut-off; permporometry, biliquid; thermoporometry; microporous and porous membranes

Introduction

The main purpose of characterization is the prediction of the performance (flux and rejection) of a membrane from its morphological properties. Complete characterization demands an understanding of the performance properties of the membrane in close relation to the characteristic data for the membrane structure and no one method can fulfill this requirement. A number of methods such as molecular weight cut-off (MWCO) determination [1–6], electron microscopy [7–16], thermoporometry [4,17–20], combined bubble pressure and solvent permeability method (biliquid permporometry) [21–26], and permporometry [27,28]

*Paper presented at the Int. Membrane Science and Technology Conference, November 10–12, 1992, Sydney, Australia.

**To whom correspondence should be addressed.

SSDI 0376-7388(93)E0044-K

have been considered for evaluation of pore characteristics. However, the individual techniques have been used in isolation by research groups under different experimental conditions. This has resulted in difficulties in assessing or comparing data as follows:

(i) For a given membrane the information is often dependent on the protocol used such as the type of solvent and solute, etc.

(ii) It is difficult to compare membranes from different manufacturers since the separation characteristics given are often based on experiments using different test molecules under different operating conditions.

(iii) Although much data are available using different techniques in the literature, there are limitations for the comparative study due to differences in chemical properties of the membrane and experimental conditions.

(iv) Variability in membranes can be significant, even within the same batch of membranes [7].

This paper aims to give a truly comparative study of the techniques using the same types of membrane to identify the limitations of the techniques. The techniques compared in this work are thermoporometry, MWCO determination and the biliquid permporometry. Data obtained from FESEM micrographs [9] using image analysis are also included for comparison.

Experimental

Membranes

The membranes used are listed in Table 1, and Fig. 1 shows field emission scanning electron micrographs (FESEM) of some membrane surfaces.

Methods

MWCO determination

All ultrafiltration (UF) experiments were performed in a thin channel module described in Ref. [29] with an effective membrane area of 37 cm^2, adjustable feed flow, and pressure. Prior to a UF experiment, distilled water was circulated in the test loop until steady state. When steady state was reached in UF, the concentrations of the bulk and permeate were analysed with a differential refractometer, Waters model R-403.

Measurements were carried out with dextrans of FL 3500, FDR 5200, T10, T40, T70 and T500 and poly(ethylene glycol)s (PEG) with average molecular weights of 600, 1000, 1500, 2000, 3000, 10,000, 20,000, and 35,000 obtained from Pharmacia, Uppsala, Sweden and Merck, Schuchardt, Germany respectively. In MWCO determination, while single solute (dextran or PEG) was used for tight membranes (PM30, YM30), for more open membranes (PTHK, MPS) both PEG and dextran were used due to unattainability of PEG in high molecular weight range. The test solutions were prepared by dissolving preweighed amounts of dextran or PEG in salt-free distilled water at a concentration of 1.5 g/l. Test conditions were pressures of 50, 100 and 200 kPa, feed recirculation rate, $U=1.87$ m/sec with Reynolds number 3700. The circulation velocity was regulated by a pump.

Most often nominal MWCO values given by manufacturers are based on observed (apparent) rejection, $R_a=(C_b-C_p)/C_b$ (where C_p is permeate concentration, C_b is bulk concentration) which differs significantly from true rejection, $R_t=(C_m-C_p)/C_m$ (where C_m is wall concentration) because of higher solute concentration at the membrane surface than that in the bulk due to concentration polarization. From the film theory model the following relationship [30] can be derived in order to calculate the true rejection from the apparent rejection,

$$\ln[(1-R_a)/R_a)]=\ln[(1-R_t)/R_t]+J_v/K \quad (1)$$

TABLE 1

Membranes used

Membrane	Manufacturer	Polymer material	Nominal mol.wt. cut-off (Da)
YM3	Amicon	Regenerated cellulose	3,000 (2.6 nm)[a]
PM30	Amicon	Polysulfone	30,000 (7.9 nm)
YM30	Amicon	Regenerated cellulose	30,000
YM100	Amicon	Regenerated cellulose	100,000 (14.1 nm)
PTHK	Millipore	Polysulfone	100,000
MPS	Memtec	Polysulfone	100,000

[a]Figures in brackets are estimated diameters from the nominal MWCO values using the Stokes-Einstein equation (see eqn. (2), where $D=8.76\times10^{-4}$ (mol.wt.)$^{-0.48}$ [30]).

where $C_m=(C_b-C_p)\exp(J_v/K)+C_p$ and K (mass transfer coefficient) is estimated from $K=(DA/d_h)Re^{0.8}Sc^{0.33}$. The diffusion coefficient D was calculated from the Stokes-Einstein correlation,

$$D=kT/(6\pi\mu r_s) \quad (2)$$

where the radius r_s of different solutes used are in Ref. [31] and k is the Boltzman constant. The coefficient A is taken as 0.023.

Biliquid permporometry

Membranes were washed according to the manufacturer's instructions. A set of immiscible liquids were prepared as follows: Distilled water-mixture of isobutanol, methanol and water (15:7:25 v/v) ($\delta=0.35$ mN/m [23]). Prior to measurements, all membranes were conditioned with solution 'A' (better wetting agent than 'B') under vacuum. While regenerated cellulose (YM30, YM100) membranes were saturated with water, the alcohol mixture was used for polysulfone membranes (PM30, PTHK, MPS). Equilibrium flux of the displacing fluid (water; PM30, PTHK, MPS, alcohol mixture; YM30) was recorded as a function of pressure. No membrane swelling was observed.

For calculation, assuming cylindrical pores the Hagen-Poiseuille relationship can be used,

$$Q=(\pi\Delta P/8\mu l)\sum n_i r_{pi}^4 \quad (3)$$

where ΔP is transmembrane pressure, μ fluid viscosity, l pore length, n_i pore numbers with pore radius r_{pi}. The biliquid permporometry is based on the assumption that the saturating liquid 'A' in the pore of radius r is replaced by liquid 'B' (immiscible with 'A' and less wettability) according to the Cantor equation [3]

$$r=2\delta/\Delta P \quad (4)$$

where δ is the interfacial tension between the two liquids. The fraction permeability due to the number of pores with radius r_{pi} is given by [26],

$$f_{pi}=[\Delta(J/\Delta P)_i]/[(J/\Delta P)_{max}-(J/\Delta P)_{min}] \quad (5)$$

the fraction of active pore number is,

$$f_n=[\Delta(J/\Delta P)_i/r_{pi}^4]/[\sum\Delta(J/\Delta P)_i/r_{pi}^4]^{0.25} \quad (6)$$

and the mean pore diameter of active pores is defined by,

$$d=(128\mu l/N\pi\Delta p)^{0.25}=2(\sum f_{ni}r_{pi}^4)^{0.25} \quad (7)$$

Thermoporometry

The membrane sample was washed by soaking several times in distilled water and the excess water on the surface was carefully removed

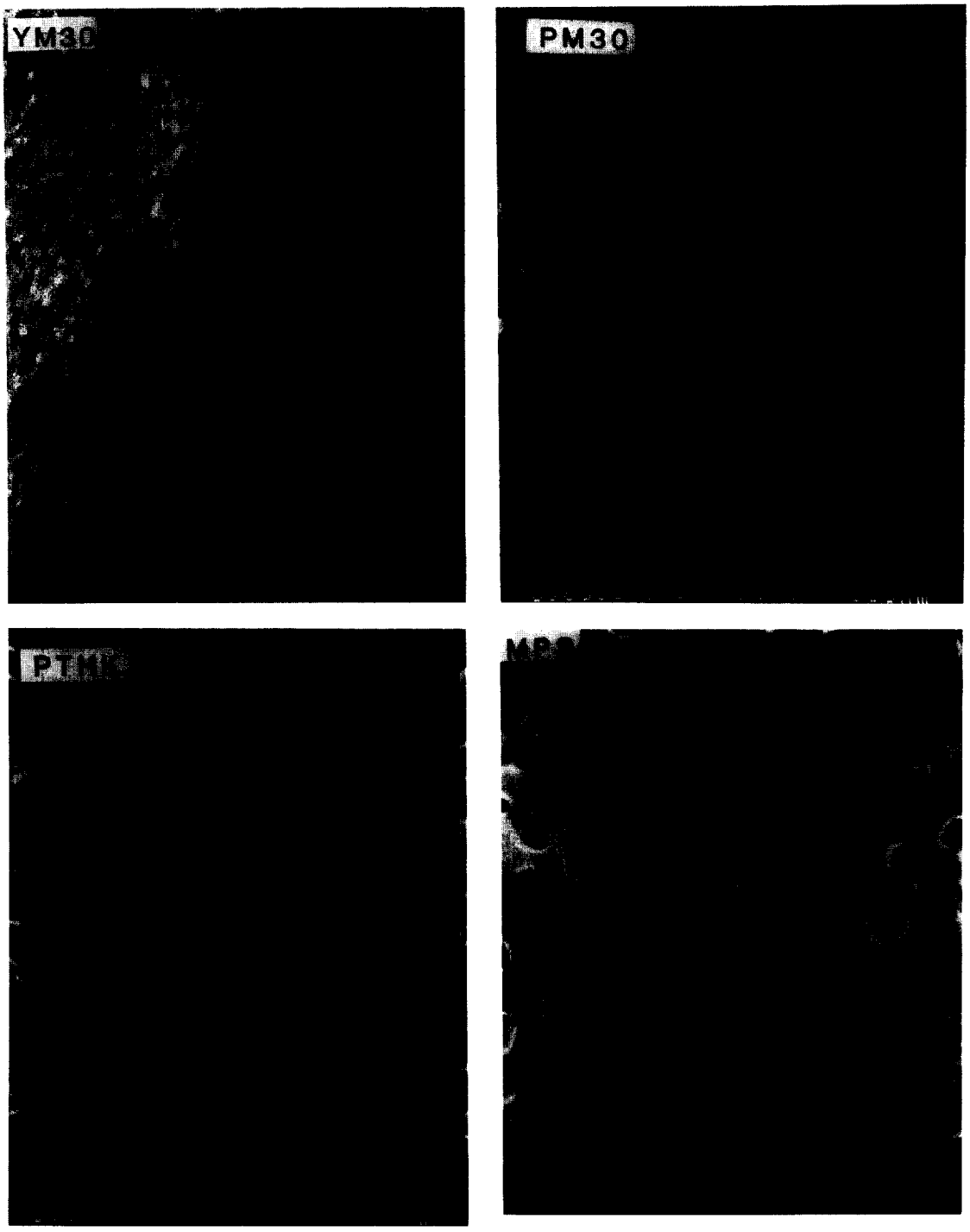

Fig. 1. SEM micrographs of membrane surfaces.

using a clean tissue. A sample (20–50 mg) (in preparation of the specimen, the backing substrate was removed from the YM100, but the backing material is included for other membranes) saturated with water was placed in a preweighed stainless pan and sealed. All the calorimetric measurements were performed with a Perkin-Elmer DSC-4 differential scanning calorimeter. Prior to heating to 10°C (283 K) with a scanning rate of 2°C/min (1 or 3°C/min was also used), the sample was cooled with a maximum speed of 320°C/min to −40°C (233 K). Differential pore volume versus pore radius was obtained by analysing the thermogram according to Brun et al. [17].

When water saturated membranes are cooled down, undercooling, ΔT [difference between a measured temperature and the triple point of water (273 K)] is related to the radius of an ice crystal r_c, and is inversely proportional to the degree of undercooling. Water in the porous media therefore crystallizes or melts at the temperature where the pore radius $r_p = r_c$. From the thermogram, the relation between the pore radius (nm), r_p and the extent of undercooling, ΔT is calculated using equations [17]:
During solidification

$$r_{ps} = (-64.67/\Delta T) + 0.57 \quad (8)$$

During fusion

$$r_{pf} = (-32.33/\Delta T) + 0.68 \quad (9)$$

From the heat effect [fusion or melting energy (J/g)] occurring during the transition, the void (pore) volume at a certain ΔT can be evaluated:
During solidification

$$W_{as} = -0.0556\Delta T^2 - 7.43\Delta T - 332 \quad (10)$$

During fusion

$$W_{af} = -0.055\Delta T^2 - 11.39\Delta T - 332 \quad (11)$$

The melting process was used for the pore size analysis in this paper; the pores corresponding to the maximum of the distribution curves $dV/dr = f(r)$ are obtained by comparing the fusion curves of the capillary condensate.

Results and discussion

Table 2 compares the mean pore diameters of the membranes (typically 2 to 3 pieces from the same batch for each membrane type) determined using the different characterization methods, and also includes the data determined from EM for comparison. Relative correspondence of the measured data can be seen for the 'different' membrane types, although the diameter obtained by each technique differs significantly for the 'same' types of membrane. The biliquid permporometry and thermoporometry methods give significantly higher values than the MWCO method. The closes comparison is obtained between the EM values and the MWCO method. This suggests that the controlling pore dimension for separation is the surface skin dimension. The largest discrepancy when comparing MWCO and EM value is for the MPS membrane, and this may be due to its different morphology (see Fig. 1) which could have controlling pore dimensions below the skin layer. However, it should also be noted that the relationship between the size of a partially rejected solute and the size of the pores is an intricate one and that even the simplest of the models predict a substantial difference between the two; Ferry's model [32] predicts the diameter of the capillary to be 1.4 times larger than the diameter of the sphere rejected at 90% level.

It is also shown that the pore diameters analyzed by the thermoporometry are substantially larger than those estimated from the biliquid permporometry. This is possibly because thermoporometry pore radii corresponding to distribution maxima have contributions from pores of comparable size both in the skin and sublayers [33] as pore size transition from the skin to sublayer is not well defined for aniso-

TABLE 2

Results measured by each characterization method

Membrane	MWCO (nm)[a]	Biliquid (nm)	Thermoporometry (nm)	EM (nm)[b]
PM30	4.1-5.9	13.5 (11.0-17.0)[c]	~24[d]	4.0
YM30	4.4-4.7	8.5 (5.9-11.1)	13.4 (11.6-15.0)	
YM100		13.3		
PTHK	4.9-7.2	27.4 (26.2-28.6)		9.2
MPS	5.1-7.4	23.3-38.2		18.9

[a]Diameter estimated from MWCO values (true rejection; see Table 3) at 50, 100 and 200 kPa, using the Stokes-Einstein equation (see eqn. (2), where $D=8.76\times10^{-4}$ (mol.wt.)$^{-0.48}$ [30]).
[b]Mean pore diameter obtained by image analysis from FESEM micrographs [9] without correcting the diameter due to coating (~2 nm thick chromium coating).
[c]Average pore diameter; Figures in brackets are range of pore diameters obtained using different membrane samples.
[d]Result is not reliable due to lack of suitability of thermoporometry for the PM30 because of low pore volume.

tropic membranes. Zeman and Tkacik [20] also observed that thermoporometry gave pore sizes of UF membranes one order of magnitude larger than those by SEM. They suggested that thermoporometry measures the pores in the sublayer of the membrane indicating that this method gives insufficient information on the pores present in the skin only. The biliquid permporometry determines the dimensions of the narrowest part of the pore (possibly the pore entrance), whereas the thermoporometry measures the effective dimension of the pore cavity (not pore opening).

For MWCO determination, cut-off values of the membranes tested under the same conditions differ significantly from nominal MWCO given by manufacturers. It is not surprising, as different manufacturers use different type of solutes (proteins, dextrans, PEG, etc.) as well as different test conditions (pressure, feed velocity, concentration, pH, temperature, geometry of the test cell, etc.). In addition, cut-off values are not only strongly influenced by operating parameters, but also controlled by other factors such as concentration polarization and fouling.

MWCO determination

The typical apparent and true rejection curves for PM30 and YM30 membranes at 50 kPa, as a function of molecular weight, are shown in Fig. 2. The PM30 and YM30 have the same nominal MWCO (=30 kDa), but they are composed of different material (see Table 1). The curves for the PM30 are sharper than those for the YM30. While the cut-off level of the membrane depends on its mean pore size, the sharpness of cut-off depends on the breadth of the pore size distribution. When the curves ob-

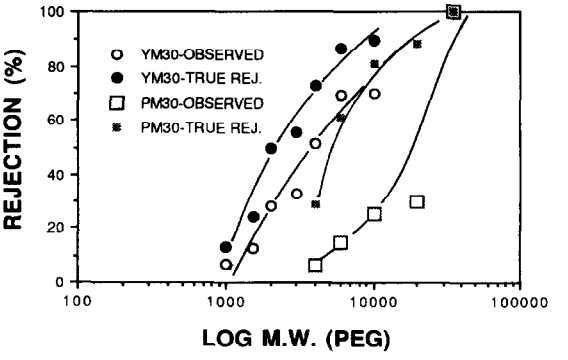

Fig. 2. Rejection characteristics of PM30 and YM30 membranes at 50 kPa.

tained from observed and apparent rejections are compared, the PM30 membrane shows larger deviations than the YM30, indicating a fouling effect on the PM30 membrane (see below for further discussion). In general, thinner and less diffusive membranes tend to show sharper cut-offs.

Since the pressure has different effects on different membranes, the membrane rejection was determined at different pressures of 50 kPa, 100 kPa and 200 kPa and typical true rejection (corrected for concentration polarization) curves for PM30 membranes are presented in Fig. 3. The cut-off values measured in this experiment and defined as 90% rejection (true rejection) for dextran or PEG molecules ar summarized in Table 3. Except for the YM30, the cut-off value for all membranes increases as

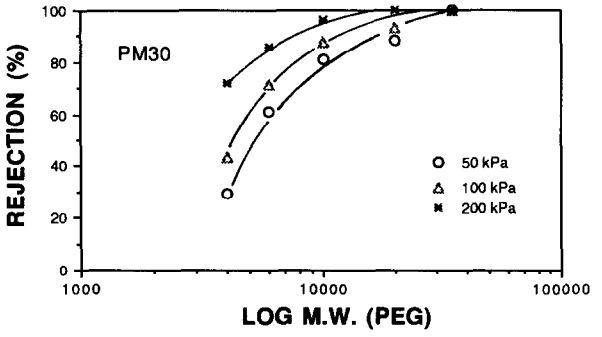

Fig. 3. Rejection characteristics of PM30 membranes at different transmembrane pressures.

TABLE 3

Measured MWCO values obtained from true rejection using PEG and dextran

Membrane	Transmembrane pressure (kPa)			Remarks
	50	100	200	
YM30	10,000 Da	10,000 Da	9,000 Da	
PM30	14,000	11,300	7,500	PEG
	16,500	13,500	7,500	Dextran
PTHK	25,000	16,000	11,000	
MPS	26,000	20,000	13,800	

transmembrane pressure decreases. Little effect of pressure for the hydrophilic YM30 membrane indicates that the differences for the PM30 are due to fouling. If the assumptions used for the MWCO determination are correct, there should be no effect of pressure for the true rejection values as they were corrected for concentration polarization. Noting that eqn. (1) is supposed to correct for concentration polarization, possible reasons for the discrepancies are as follows:

(i) The equation $K=(DA/d_h)Re^{0.8}Sc^{0.33}$ is not giving a correct prediction of K. However, this is unlikely to be a major cause for the difference, as the equation provides a good prediction for the less fouling YM30 membrane.

(ii) The correction assumes a mono-sized solute, whereas dextrans have a 'mean' molecular weight and a distribution. The large molecules in the distribution could form a barrier to transmission which is not accounted for by the correction – this could be exacerbated at higher ΔP, giving less transmission, i.e. more rejection as ΔP increases.

(iii) Solutes deform or distort in the region of pores [34] – this would be function of J_v (and hence ΔP).

Table 3 also includes results obtained using different solutes (dextran and PEG) for PM30 membranes. PEG resulted in slightly lower cut-off values than dextran. PEG is reported to have larger hydrodynamic diameter [31] than dextran. However, the difference could also be attributed to differences in the molecular weight distribution of the two solutes or to differences in interactions between the solute and the membrane.

The overall observation is that the comparison of the membranes tested under the same test conditions yielded results that differ remarkably from the manufacturers supplied cut-off values (see Table 1). Table 3 illustrates how MWCO can lead to misunderstanding and misinterpretation in actual processes, unless con-

ditions are specified due to the strong influence of operating parameters.

Biliquid permporometry

Figure 4 compares the active pore size distributions of the UF membranes measured in this study. The regenerated cellulose membranes (YM30 and YM100) have much narrower distributions than the polysulfone membranes (PM30, PTHK and MPS), which contradicts the sharper rejection curve (Fig. 2), indicating that the broader distribution of the YM30 (Fig. 2) was controlled by the diffusive character of the regenerated cellulose membrane.

The detection of large pores in the PM30 membrane determined by the biliquid permporometry is consistent with greater MWCOs [i.e. low rejection (see Table 3)] obtained by the MWCO determination.

Thermoporometry

Because eqns. (9) and (11) used for analysis of thermograms are based on the assumption of solid–liquid thermodynamic equilibrium, thermograms were obtained at scanning rates of 1°C/min, 2°C/min and 3°C/min (Fig. 5a). The corresponding pore volume distribution

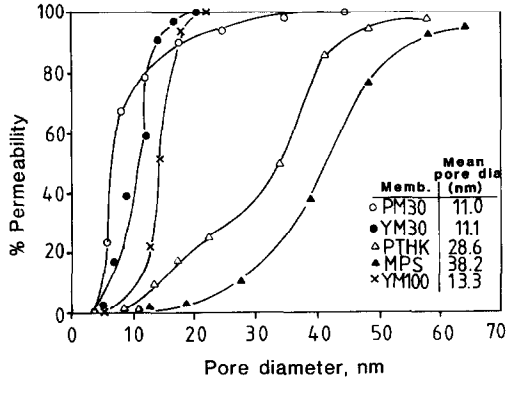

Fig. 4. Pore size distributions of UF membranes obtained using biliquid permporometry.

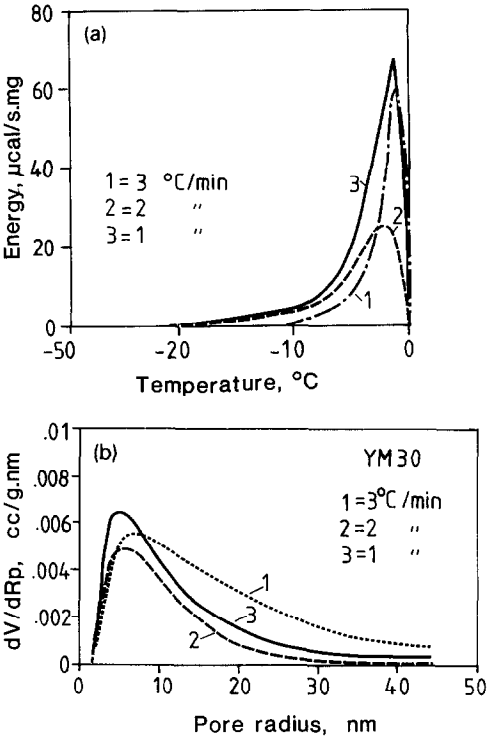

Fig. 5. (a) Effect of scanning rate on thermograms of YM30 membranes. (b) Effect of scanning rate on pore volume distribution curves (calculated from Fig. 5(a)) for YM30 membranes.

curves calculated from the data of Fig. 5(a) are shown in Fig. 5(b). It is clear from Fig. 5(a) that the 3°C/min scan was not performed under equilibrium conditions. The change of temperature was too rapid to detect freezing of water in very small pores; note that the change of temperature with the 3°C/min scan occurs at much higher temperature (about −10°C) than those (about −20°C) with slower scan rates of 1 and 2°C/min. All membranes were therefore characterized with a scanning speed of 2°C/min.

Figure 6 represents typical thermograms for regenerated cellulose (Fig. 6a) and polysulfone (Fig. 6b) membranes. In Fig. 6(a), while peak 1 (left) represents the melting of ice in the pores of the membrane, peak 2 which starts at ap-

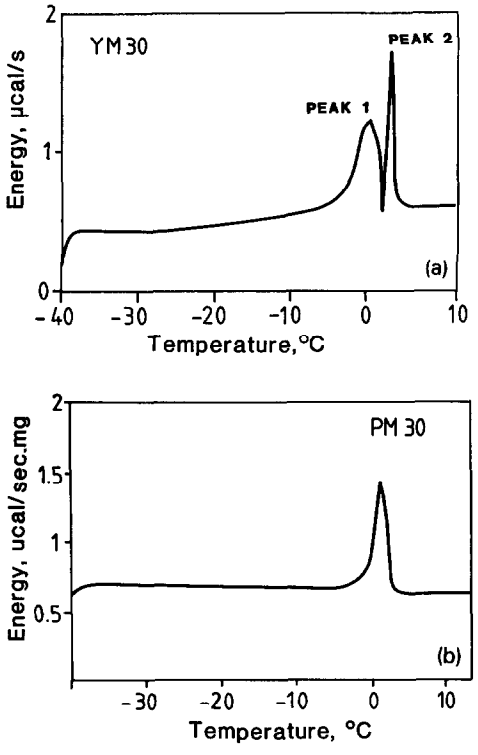

Fig. 6. (a) Typical experimental thermogram of regenerated cellulose membrane. (b) Typical experimental thermogram of polysulfone membrane (PM30).

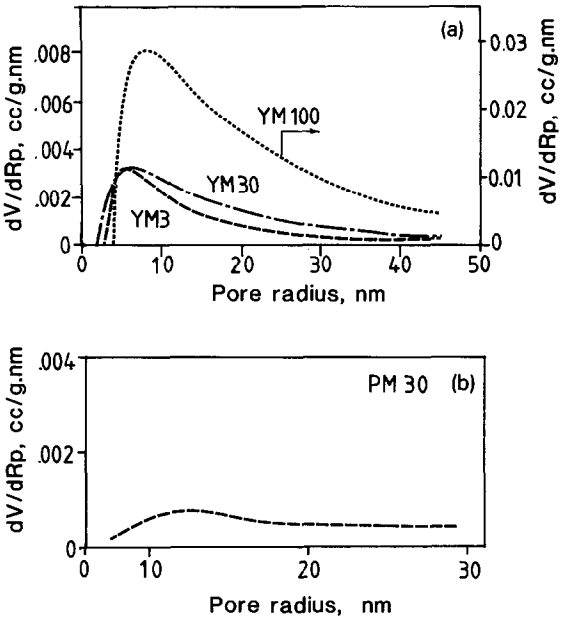

Fig. 7. (a) Pore volume distribution curves of regenerated cellulose membranes (YM3, YM30 and YM100) with varying MWCO values. (b) Pore volume distribution calculated from thermogram shown in Fig. 6(b) for PM30 membrane.

proximately 0°C is due to the melting of the normal ice of free water [35,36] adhering to the membrane wall or in the substrate. In contrast to the YM30 (Fig. 6a) with two peaks, the PM30 (Fig. 6b) shows only one peak. The reason for the lack of the first peak for PM30 is unknown. However, one possibility could be that the more hydrophobic polysulfone material of the PM30 has less water bound to the pore walls. Analysis of thermograms yielded pore volume distributions presented in Fig. 7. Estimated pore sizes (Fig. 7a), (see also Table 2) for regenerated cellulose membranes showed a progressively increasing trend with an increase in nominal MWCO values. As seen in Fig. 7(b), results for polysulfone membranes were not so successful. The PM30 thermogram does not show any changes in energy at low temperature (i.e. in the small pores) resulting in the pore diameters of about 8 nm and 60 nm for the smallest and the largest pores respectively, which are significantly larger than the reported pore size [9] by EM observation. This was possibly caused by the very low pore volume due to the thin skin layer and the extremely low surface porosity [8,9,11] as well as their much poorer wettability to water than the regenerated cellulose membranes.

Conclusions

Despite the claim that MWCO determination has the closest resemblance to real operating conditions the characterization data for porous membranes often lead to misunderstanding and misinterpretation due to differences for different types of solute, the membrane system and the process parameters used.

For 'fixed operating conditions' a determination and comparison of the rejection curves of different UF membranes can easily be achieved. However, the MWCO values alone cannot fulfill the requirements for membrane characterization, as the cut-off is not only strongly influenced by transmembrane pressure difference, but is also very sensitive to slight deviations in the rejection curve.

Thermoporometry can provide limited information ('relative' pore size or size distribution) on certain types of polymer UF membranes which are saturated completely by the solvent used (water in this work). The data obtained by thermoporometry are much greater than those by the biliquid permporometry due to the existence of comparable pores in both skin and sublayers because of the indistinct transition layer for anisotropic membranes.

Except for regenerated cellulose membranes, all membranes produced quite a wide permeability curve due to significant contributions from large pores (even in small numbers). The biliquid permporometry also involves uncertainties arising from the pore length and contact angle between the membrane permeating fluids.

Mathematical models used for each technique are rather oversimplified for the actual conditions of the membranes. The techniques can however complement each other and provide useful information on the final properties and performance of the membranes. While the characterization by MWCO determination gives information on the separation properties, biliquid permporometry and thermoporometry are useful tools for the evaluation of pore size distribution.

Acknowledgement

This work was financially supported by the Department of Industry, Technology and Commerce, Australia for K.J. Kim to visit the University of Technology, Compiègne (France), the Technical University of Denmark, and the University of Twente (The Netherlands) for the use of facilities for the biliquid displacement, MWCO determination, and thermoporometry, respectively.

List of symbols

A	membrane area (m^2)
C_b	solute concentration in the bulk (g/l)
C_m	solute concentration at membrane surface (g/l)
C_p	solute concentration in the permeate (g/l)
d	mean pore diameter
D	diffusion coefficient (m^2/sec)
d_h	equivalent hydraulic diameter (cm)
f_{pi}	fraction permeability due to the number of pores with radius r_{pi}
f_n	fraction of active pore number
J_v	flux (l/m^2-hr)
k	Boltzman constant
K	mass transfer coefficient
l	pore length (assumed to be equal to the thickness of the skin layer) (cm)
N	number of pores
n_i	pore numbers with pore radius r_{pi}
ΔP	transmembrane pressure (Pa)
r	pore radius (angstrom)
r_s	radius of solute (cm)
R_a	apparent rejection
R_t	true rejection
Re	Reynolds number
Sc	Schmidt number
T	temperature (K)
u	velocity (m/sec)
V	pore volume (cm^3/g)
W_{af}	apparent energy of fusion (J/g)
W_{as}	apparent energy of solidification (J/g)
δ	interfacial tension between two liquids (mN/m)
μ	effluent fluid viscosity (poise)

References

1 R.E. Kesting, Synthetic Polymer Membranes, McGraw Hill, New York, NY, 1971.
2 G. Jonsson, Molecular weight cut-off curves for ultrafiltration membranes of varying pore sizes. Desalination, 53 (1985) 3-10.
3 G. Trägårdh and K. Olund, A method for characterization of ultrafiltration membranes, Desalination, 58 (1986) 187-198.
4 C.A. Smolders and E. Vugteveen, New characterization methods for asymmetric ultrafiltration membranes, in: D.R. Lloyd (Ed.), Material Science of Synthetic Membranes, ACS Symp. Ser., 269 (1985) 327-338.
5 M. Cheryan, Ultrafiltration Handbook, Technomic Publication Co. Inc., Lancaster, USA, 1986.
6 J.H. Hanemaaijer, T. Robbertsen, Th. van den Boomgaard, C. Olieman, P. Both and D.G. Schmidt, Characterization of clean and fouled ultrafiltration membranes, Desalination, 68 (1988) 93-108.
7 A.G. Fane, K.J. Kim, C.J.D. Fell and A. Suki, Characterization of ultrafiltration membranes: flux and surface properties, Workshop on characterization of ultrafiltration membranes, Orenas Slott, Sweden, Swedish Foundation for Membrane Technology, 1987, pp. 39-80.
8 A.G. Fane, C.J.D. Fell and A.G. Waters, The relationship between membrane surface pore characteristics and flux for ultrafiltration membranes, J. Membrane Sci., 9 (1981) 245-262.
9 K.J. Kim, A.G. Fane, C.J.D. Fell, T. Suzuki and M.R. Dickson, quantitative microscopic study of surface characterization of ultrafiltration membranes, J. Membrane Sci., 54 (1990) 89-102.
10 K.J. Kim, A.G. Fane and C.J.D. Fell, Fouling mechanisms of membranes during protein ultrafiltration, J. Membrane Sci., 68 (1992) 79-91.
11 U. Merin and M. Cheryan, Ultrastructure of the surfaces of polysulfone ultrafiltration membranes, J. Polym. Sci., 25 (1989) 2139-2142.
12 F. Martínez-Villa, J.I. Arribas and F. Tejerina, Quantitative microscopic study of surface characterization of track-etched membranes, J. Membrane Sci., 36 (1988) 19-30.
13 A. Kakuta, M. Kuramoto and M. Ohno, Freeze-dried cellulose acetate membrane fine structure observation, J. Polym. Sci., 18 (1980) 3220-3243.
14 H.J. Preusser, Die Ultrastruktur einiger feinporiger Membranfiltertypen, Kolloid, Z. u. Z. Polymere, 250 (1972) 133-141.
15 R.D. Schultz and S.K. Asunmaa, in: J.F. Danielli, A.C. Riddiford and M. Rosenberg (Eds.), Recent Progress in Surface Science, Vol. 3, Academic Press, New York, NY, 1970, pp. 291-332.
16 K. Chan, T. Matsuura and K. Rajan, Determination of pore sizes at the skin layer of aromatic polyimohydrazide ultrafiltration membranes, J. Polym. Sci., 21 (1983) 417-422.
17 M. Brun, A. Lallemand, J.F. Quinson and C. Eyraud, A new method for the simultaneous determination of the size and shape of pores: thermoporometry, Thermochim. Acta, 21 (1977) 59-88.
18 J.F. Qinson, H. Kral and M. Brun, Progress in thermoporometry, in: K.K. Unger, J. Rouquerol, K.S.W. Sing and K. Kral (Eds.), Characterization of Porous Solids, Elsevier, Amsterdam, 1988, pp. 307-315.
19 A. Higuchi, J. Komiyama and T. Iijima, The states of water in gel cellophane membranes, Polymer Bull., 11 (1984) 203-208.
20 L. Zeman and G. Tkacik, Characterization of porous sublayers in UF membranes by thermoporometry, J. Membrane Sci., 32 (1987) 329-337.
21 K. Kamide and S. Manabe, Characterization technique of straight-through porous membrane, in: A.R. Cooper (Ed.), Ultrafiltration Membranes and Applications, Plenum Press, New York, NY, 1980, pp. 173-202.
22 S. Munari, A. Bottino, G. Capannelli and P. Moretti, Membrane morphology and transport properties, Desalination, 53 (1985) 11-23.
23 G. Capannelli, F. Vigo and S. Munari, Ultrafiltration membranes - Characterization methods, J. Membrane Sci., 15 (1983) 289-313.
24 M. Zeni, I.R. Bellobono, F. Muffato, A. Polissi, E. Selli and E. Rastelli, Photosynthetic membranes. VI. Characterization of ultrafiltration membranes prepared by photografting zeolite-epoxy-diacrylate resin composites onto cellulose, J. Membrane Sci., 36 (1988) 277-295.
25 S. Munari, A. Bottino, P. Moretti, G. Capannelli and I. Becchi, Permporometric study on ultrafiltration membranes, J. Membrane Sci., 41 (1989) 69-86.
26 R. Kerbage, M.M. Peuchot and R. Ben Aim, Evolution de l'afficacite des membranes par la mesure de distribution des pores actifs, Recents Progrès en Genie des Procedis, 5-15 (1991) 61-66.
27 M. Katz and G. Baruch, New insights into the structure of microporous membranes obtained using a new pore size evaluation method, Desalination, 58 (1986) 199-211.
28 A. Mey-Marom and M.G. Katz, Measurement of active pore size distribution of microporous membranes

- A new approach, J. Membrane Sci, 27 (1986) 119-130.
29 G. Jonsson, Concentration polarization in a reverse osmosis test cell, Desalination, 21 (1977) 1-10.
30 G. Jonsson and C.E. Boesen, Polarization phenomena in membrane processes, in: G. Belfort (Ed.), Synthetic Membrane Processes, Academic Press, New York, NY, 1984, Chap. 4, pp. 101-130.
31 G. Jonsson and P.M. Christensen, Separation characteristics of ultrafiltration membranes, in: E. Drioli and M. Nakagaki (Eds.), Membranes and Membrane Processes, Plenum Press, New York, NY, 1986, pp.179-190.
32 J.D. Ferry, Ultrafilter membranes and ultrafiltration, Chemical Review, 18 (12) (1936) 373-455.
33 F.P. Cuperus, D. Bargeman and C.A. Smolders, Critical points in the analysis of membrane pore structures by thermoporometry, J. Membrane Sci., 66 (1992) 45-53.
34 S. Mochizuki and A. Zydney, Dextran transport through asymmetric ultrafiltration membranes: Comparison with hydrodynamic models, J. Membrane Sci., 68 (1992) 21-41.
35 H.G. Burghoff and W. Push, Characterization of water structure in cellulose acetate membranes by calorimetric measurements, J. Appl. Polym. Sci., 23 (1979) 473-484.
36 Y. Taniguchi and S. Horigome, The state of water in cellulose acetate membranes, J. Appl. Polym. Sci., 19 (1975) 2743-2748.